

## A spectral element method for unsaturated flow in porous soils

ERNEST LÉONTIN LEMOUBOU

Life & Industrial Systems Thermal Engineering-Team (LISTE-T)  
Unité de Recherche de Mécanique de Modélisation des Systèmes Physiques (UR2MSP)  
Department of Physics  
University of Dschang  
P.O. Box 67 Dschang, Cameroon  
CAMEROON  
[ernestlemoubou@yahoo.fr](mailto:ernestlemoubou@yahoo.fr)

HERVE THIERRY TAGNE KAMDÉM

Life & Industrial Systems Thermal Engineering-Team (LISTE-T)  
Unité de Recherche de Mécanique de Modélisation des Systèmes Physiques (UR2MSP)  
Department of Physics  
University of Dschang  
P.O. Box 67 Dschang, Cameroon  
CAMEROON  
[herve.kamdem@univ-dschang.org](mailto:herve.kamdem@univ-dschang.org)

JEAN ROGER BOGNING

Department of Physics  
University of Bamenda  
CAMEROON  
[jrbogning@yahoo.fr](mailto:jrbogning@yahoo.fr)

MYRIAM LAZARD

Laboratoire Pprime-UPR3346  
Université de Poitiers  
FRANCE  
[myriam.lazard@univ-poitiers.fr](mailto:myriam.lazard@univ-poitiers.fr)

EDOUARD HENRI ZEFACK TONNANG

International Institute of Tropical Agriculture (IITA)  
08 BP 0932 Abomey, Calavi, Cotonou, Benin  
BENIN  
[htonang@gmail.com](mailto:htonang@gmail.com)

*Abstract:* - A spectral element method for one-dimensional transient water flow in unsaturated soils considering the pressure head form of the Richards flow equation is developed. The analyses were performed for pressure head flow in horizontal, upward and downward vertical unsaturated soils and for various hydraulic characteristics. The spectral element method combines the flexibility of the finite element method with the accuracy of spectral techniques. The spatial discretized equation was performed using the Galerkin weighted formulation combined with Legendre Gauss-Lobatto quadrature sets, whereas the temporal discretization is achieved by the Picard iteration procedure for soil moisture linearization combines with fully implicit time three-level scheme and two-level scheme with/without standard chord slope. The spectral element predictions compare well with exact results for pressure head flow in horizontal, upward and downward vertical unsaturated soils. The spectral element method results also compare favorably with the finite element method with mass-lumped approximation. Numerical experiments indicated that the spectral element method with standard chord

slope schemes is mass conservative: the mass balance error is zero for different soil types considered. The numerical experiments also show that the spectral element method with three level scheme is more efficient than if using standard two-level scheme. Finally, it is found that the spectral element method is a convergent algorithm, which maintains high accuracy and less computational times. The present formulation of the spectral element method for unsaturated flow problem is original and it is of special importance for soil hydrology and groundwater management.

*Key-Words:* - Hydraulic characteristics, numerical experiments, Richards flow equation, soil moisture prediction, spectral element method, unsaturated soils

## 1 Introduction

Water flow processes cover some of the most important challenges of our time because it is the keys to acquire general knowledge on groundwater movement, quantify limits, soil-atmosphere processes such as rainfall, interception, infiltration, soil moisture redistribution and root water uptake [1-3]. Flow processes can be conveniently classified in two groups: saturated flows for water-table and unsaturated flows above the water-table. The water flow processes that occur in unsaturated soil substantially contribute to a wide variety of hydrologic processes [4-6]. In fact, water flow in unsaturated soil is greatly influenced by unsaturated hydrostatics phenomena such as water content, pressure gradient, retention and energy transfer. It is also influenced by unsaturated hydrodynamics phenomena named diffuse flow or infiltration and preferential flow [7-11]. Study of this phenomenon requires proper modeling of the governing equations and constitutive relation involves.

Flow process through unsaturated soil is governed by the fundamental Richards equation [12,13]. This equation is commonly presented in three forms: pressure, moisture and mixed pressure-moisture partial differential forms [14,15]. The pressure-based Richards flow equation is considered to be more useful for practical problems since it facilitates modeling of soil systems that are locally saturated and it provides a state variable that is always continuous in space [16,17]. However, this flow equation can lead to large mass balance errors [15,16,18]. This problem, which has been linked to the expansion of the storage term, can be circumvented by decreasing the variability of the storage coefficient during the time step within an element space size, evaluates the storage coefficient as an effective, or average value over element and the duration of the time step, or when equivalence in the expansion of the storage term is maintained in the discretized form. These principles have been applied successfully using finite difference (FDM)

method [16], finite element (FEM) method [17-21] and finite volume (FVM) method [22].

In the current research, a spectral element method (SEM) is presented to predict the pressure head in unsaturated porous soils characterized by variable moisture content capacity and hydraulic conductivity, which induce nonlinearity effects in the mathematical model. In developing the method, the spatial discretized equation is performed using the Galerkin weighted formulation combined with Legendre Gauss-Lobatto quadrature sets, whereas the temporal discretization is achieved by the Picard iteration procedure for soil moisture linearization combines with fully implicit time schemes with/without standard chord slope. The SEM was first proposed by Patera [23] for finding numerical solutions of the incompressible fluid flow equations. It is an approach with dual features that combines the flexibility of the finite element method with the accuracy of spectral techniques. In fact, FEM has been widely applied in complex engineering domains because it is flexible to capture solution for complex geometry problems [24,25]. However low order FEM often presents some weaknesses to perfectly capture some complex solution characteristics [24-27]. The spectral element technique has been successfully developed based on Chebyshev polynomials and Lagrange interpolation combined with Gauss-Lobatto-Legendre quadrature to improve computational efficiency of finite element methods. The use of the Gauss Lobatto quadrature approach leads to a diagonal mass matrix which greatly accelerates the convergence rate of the method [26]. It has been mostly used in many branches of science and engineering especially for linear and homogeneous problems. Komatitsch et al. [27] presented a spectral element solution of the wave propagation near fluid interface. Their study emphasized on the simplicity and the efficiency of the method to deal with strong topography at the fluid-solid interface. Shamsi [28] provided a methodology with the modified pseudo spectral scheme for accurate solution of Bang-Bang optimal

control problems. Ben-yu Guo et al. [29] considered the problem of Dirac equation and provided a solution with Hermite pseudo-spectral approach. Chen et al. [30] solved the problem of free surface viscous flows using Pseudospectral element model. Dehghan and Sabouri [31] presented a solution to the predator-prey system with interacting populations. El-Baghdady et al. [32] also studied the convection-diffusion equation, one dimensional parabolic advection-diffusion equation with constant parameter subject to a given initial and boundary conditions. Minjeaud and Pasquetti [33] demonstrated the development of the spectral element schemes for high order partial differential equations. The SEM has been shown to be very attractive in terms of accuracy, computational efficiency, and suitability to parallel computation. A number of software packages such as Semtex, Nektar++, have been developed [34] to facilitate the application of the SEM technique in solving problems. Although these solvers cover an important range of application areas, they are limited with the issue of estimating the parameters of equations. Despite the prominence use of the method in physical and industrial context, the developments of the SEM have been mostly applied to resolve problems with constant and linear coefficients of permeability.

The focus of the present work is the development of the SEM to one-dimensional transient water flow in unsaturated soil with variable coefficients, which to the best of the authors' knowledge has never been formulated before in the literature. Nonlinear problems are generally solved by iterative schemes, and the standard SEM does not support directly adaptive polynomial order during time advancement. The present study, managed to provide an accurate, efficient and robust solution method that guarantees convergence rate and mass balance. Overall, the one-dimensional pressure head form of the Richards flow equation is considered for the study. The analysis has been limited to one-dimensional transient water flow in unsaturated soils in order to focus attention on the efficiency of the SEM for a physical model general used for soil moisture prediction. The computational expense and risk of non-convergence of the numerical strategy due to nonlinearity of capacity and hydraulic conductivity terms, and the presence of both diffusion and advection are the major difficulty presented in the moisture flow equation. The capability of the spectral element method to rapidly conserve mass is investigated for different soil types, flow orientations, initial and boundary conditions, and for three time steps discretization:

two-level with and without the standard chord slope (SCS) and three-level finite difference schemes.

## 2 Mathematical modeling

The computational complexity in analyzing multi-dimensional transient water flow in unsaturated soil with variable coefficients is enormous. For this reason, idealized transport models have been constructed which include simplifying assumptions. The one-dimensional transient water flow in unsaturated soil with variable coefficients is considered in this study. This problem is of great interest in many soil sciences, civil engineering and remote sensing problems [35-37]. In addition, accurate predictions of the one-dimensional transient water flow in unsaturated soil with variable coefficients using improved method as dedicated in this work may be useful for non-soil mechanics experts such as biologist, physiologist and agronomist in designing remote sensing models for a better knowledge of soil characteristics. It can also set the basis to help guide the development of more comprehensive models and codes of the complete unsaturated flow problem.

### 2.1 Water flow in unsaturated soil

The one-dimensional pressure equation used in this study was derived by considering the hydraulic properties such as the hydraulic conductivity and the specific water capacity that depend strongly on the water content. However, the fluid is assumed to be incompressible and stable. The Darcy's law [38] and the continuity equation are further considered in the development of the model. Thus, assuming that the air phase and the vapor transfer have negligible effects on the net water transfer, the equations for incompressible vapor flow and liquid flow can be combined and reduced to a generalized equation. Therefore, the one-dimensional water flow in isothermal unsaturated soil may be written in terms of the pressure head as [15]

$$C(\Psi) \frac{\partial \Psi}{\partial t} = \frac{\partial}{\partial z} \left( K(\Psi) \frac{\partial \Psi}{\partial z} \right) + \lambda \frac{\partial K(\Psi)}{\partial z} \quad (1)$$

where  $\Psi$  is the pressure head (cm),  $t$  is the time (s),  $z$  denotes the distance from the soil surface downward (cm),  $C$  is the specific water content capacity ( $cm^{-1}$ ),  $K$  is the hydraulic conductivity ( $cm \cdot s^{-1}$ ). The parameter  $\lambda$  is the unitless parameter which determines the direction of soil moisture flow; its value taken -1, 0 and 1 for downward, horizontal and upwards flow directions, respectively.

Boundary conditions for the solution of the unsaturated water flow equation, Eq. (1), are given by

$$\Psi(z = 0, t) = \Psi_0 \quad (2)$$

$$\Psi(z = L, t) = \Psi_L \quad (3)$$

and the initial condition is

$$\Psi(z, t = 0) = \Psi_i \quad (4)$$

### 2.1 Hydraulic properties of unsaturated soil

The specific water content capacity and the conductivity are needed to solve the water flow equation. The specific water content capacity is linked to the soil moisture content by

$$C(\Psi) = \frac{d\eta}{d\Psi} \quad (5)$$

where  $\eta$  is the soil moisture content ( $cm^3/cm^3$ ). Several models of the hydraulic conductivity and soil moisture content have been proposed in the literature for the hydraulic conductivity including:

#### 2.1.1 Gardner [39] model

This author proposed soil characteristics suitable for analytical solution of the water flow in saturated and unsaturated soils. The soil moisture content and the soil hydraulic conductivity are expressed, respectively, as [39,40]

$$\eta = \eta_r + (\eta_s - \eta_r)e^{-\nu\Psi} \quad (6)$$

$$K(\Psi) = K_s e^{-\nu\Psi} \quad (7)$$

where  $K_s$  is the saturated hydraulic conductivity ( $cm/s$ ),  $\eta_s$  is the saturated water content ( $cm^3/cm^3$ ),  $\eta_r$  is the residual water content ( $cm^3/cm^3$ ), and  $\nu$  is the pore size distributed parameter.

#### 2.1.2 Haverkamp et al. [41] model

The soil moisture content and the soil hydraulic conductivity are expressed in term of soil pressure head using empirical relations

$$\eta(\Psi) = \frac{\alpha(\eta_s - \eta_r)}{\alpha + |\Psi|^\beta} + \eta_r \quad (8)$$

$$K(\Psi) = K_s \frac{\rho}{\rho + |\Psi|^\gamma} \quad (9)$$

where  $\alpha$ ,  $\beta$ , and  $\gamma$  are fitting parameters while  $\rho$  is the soil bulk density ( $g/cm^3$ ).

#### 2.1.3 van Genuchten [42] model

The soil properties were approximated as follow

$$\eta(\Psi) = \frac{\eta_s - \eta_r}{[1 + (\alpha|\Psi|)^n]^m} + \eta_r \quad (10)$$

$$\frac{K(\Psi)}{K_s} = \frac{\{1 - (\alpha|\Psi|)^{n-1}[1 + (\alpha|\Psi|)^n]^{-m}\}^2}{[1 + (\alpha|\Psi|)^n]^{m/2}} \quad (11)$$

## 3 Spectral element discretization

The spectral element method is a numerical method used to discretize ordinary or partial differential equations. The general procedure for the spectral element analysis follows three major steps [27,33]: i) transformation of the partial differential equation to an integral equation with appropriate orthogonal basis functions, ii) division of the computational domain into a series of spectral elements and approximate the field variables over each sub-domain, iii) assemblage of the contribution of each sub-domain into a global system of first order ordinary differential equations which should then be discretized in time. In the present work, the spectral element method combines the Galerkin weighted formulation with Gauss-Lobatto quadrature and Gauss-Lobatto Lagrange (GLL) basis functions that uses the quadrature points as nodes. The integration over an element using the Legendre-Gauss-Lobatto integration rule generates the exact diagonal mass matrix which greatly simplifies the implementation algorithm. The governing partial differential equation of water flow in unsaturated soil, Eq. (1) is then solved using the spectral element method. In this method, the pressure head is represented as high-order orthogonal polynomials for interpolation points as follows [26,43]

$$\Psi(z, t) \approx \sum_{i=1}^{N+1} \Psi_i(t) \Phi_i(z) \quad (12)$$

where  $N$  is the total number of elements in the spectral element domain,  $\Phi_i(z)$  are the Lobatto polynomials and  $\Psi_i(t)$  are the values of the pressure head at node  $i$  which are obtained by the Galerkin weighting formulation. The Galerkin weighting formulation of Eq. (1) over the entire solution region can be written as

$$\int_0^L \left[ C \frac{\partial \Psi}{\partial t} - \frac{\partial}{\partial z} \left( K \frac{\partial \Psi}{\partial z} \right) - \lambda \frac{\partial K}{\partial z} \right] \Phi_i(z) dz = \int_0^L R(\Psi) \Phi_i(z) dz \quad (13)$$

where  $1 \leq i \leq N$  and  $R(\Psi)$  is the residual that measures the error introduced during the spectral discretization. The integral of Eq. (13) can be broken into a sum of elemental integrals and it is rewritten as

$$\sum_{l=1}^N \int_{z_1^l}^{z_2^l} \left[ C^l \frac{\partial \Psi^l}{\partial t} - \frac{\partial}{\partial z} \left( K^l \frac{\partial \Psi^l}{\partial z} \right) - \lambda \frac{\partial K^l}{\partial z} - R(\Psi^l) \right] \Phi_i(z) dz = 0 \quad (14)$$

where  $1 \leq i \leq N$ ,  $z_2^l$  and  $z_1^l$  are the boundary points of the  $l$ th element of size  $h_l = z_2^l - z_1^l$ . The pressure

head in the  $l$ th element local approximation is next represented as high-order Lobatto polynomials for interpolation points as

$$\Psi^l(\xi, t) \approx \sum_{j=1}^{N_e} \Psi_j^l(t) \Phi_j(\xi) \quad (15)$$

where  $\Psi_j^l(t)$  is the  $j$ th local time dependent unknown coefficients,  $\Phi_j(\xi)$  are the  $j$ th Lobatto polynomial and  $N_e$  is the number of nodes per element. The map function from the  $l$ th element to the reference interval  $[-1, 1]$  and its inverse are given by affine transformations [28]

$$z(\xi) = [(z_2^l + z_1^l) + (z_2^l - z_1^l)\xi]/2, \quad \xi(z) = 2(z - z_1^l)/h_l - 1, \quad (16)$$

with  $\xi \in [-1, 1]$ . Considering Eqs. (16) for the  $l$ th element of Eq. (14) yields the following integral

$$\int_{-1}^1 \left[ \frac{h_l}{2} C^l \frac{\partial \Psi^l}{\partial t} - \frac{2}{h_l} \frac{\partial}{\partial \xi} \left( K^l \frac{\partial \Psi^l}{\partial \xi} \right) - \lambda \frac{\partial K^l}{\partial \xi} \right] \Phi_i(\xi) d\xi = \frac{h_l}{2} \int_{-1}^1 R(\Psi^l) \Phi_i(\xi) d\xi \quad (17)$$

The problem is reduced to determine the unknown vector such that the residual  $R(\Psi^l)$  is minimized. Mathematically, the residual  $R(\Psi^l)$  must be orthogonal to the weighting functions. Introducing Eq. (15) into Eq. (17) and applying the Green transformation of the second term of the left hand side, the discrete Galerkin weighting formulation for internal nodes of the  $l$ th element obtained by canceling the boundary nodes term is

$$\sum_{j=1}^{N_e} \Psi_j^l(t) \frac{2}{h_l} \int_{-1}^1 K^l \frac{\partial \Phi_j(\xi)}{\partial \xi} \frac{\partial \Phi_i(\xi)}{\partial \xi} d\xi + \sum_{j=1}^{N_e} \frac{\partial \Psi_j^l(t)}{\partial t} \frac{h_l}{2} \int_{-1}^1 C^l \Phi_j(\xi) \Phi_i(\xi) d\xi = \lambda \int_{-1}^1 \frac{\partial K^l}{\partial \xi} \Phi_i(\xi) d\xi \quad (18)$$

Finally, the discrete Galerkin weighting formulation for internal nodes of the flow equation at any time can be written in a compact matrix form as

$$[\mathbf{A}] + [\mathbf{B}] \frac{d\boldsymbol{\Psi}}{dt} = \mathbf{F} \quad (19)$$

where  $\boldsymbol{\Psi}$  is the vector of local pressure head,  $[\mathbf{A}]$  is the conductance matrix,  $[\mathbf{B}]$  is the storage matrix,  $\mathbf{F}$  is the global force vector. The element diffusion matrix, the stiffness mass matrix and the driving vector force are given respectively, by

$$A_{ij}^l = \frac{2}{h_l} \int_{-1}^1 K^l \frac{\partial \Phi_j(\xi)}{\partial \xi} \frac{\partial \Phi_i(\xi)}{\partial \xi} d\xi \quad (20a)$$

$$B_{ij}^l = \frac{h_l}{2} \int_{-1}^1 C^l \Phi_j(\xi) \Phi_i(\xi) d\xi \quad (20b)$$

$$F_i^l = \lambda \int_{-1}^1 \frac{\partial K^l}{\partial \xi} \Phi_i(\xi) d\xi \quad (20c)$$

The degenerate parabolic Richards equation is well known to have solutions with low regularity. In such case, low order finite elements are suitable for its discretization and consequently the integrals of Eqs. (20), are computed with a number of nodes  $N_e = 2$  per element and using the Gauss-Lobatto quadrature rule. This leads to the use of linear interpolation shape functions  $\Phi_i(\xi) = (1 - \xi)/2$  and  $\Phi_j(\xi) = (1 + \xi)/2$  at the first and the end-nodes, respectively [28,31]. The Eqs. (20) are performed efficiently if the capacity and conductivity are written in discretized forms as

$$C^l(\xi) \approx \sum_{i=1}^{N_e} C_i^l \Phi_i(\xi) \quad (21a)$$

$$K^l(\xi) \approx \sum_{i=1}^{N_e} K_i^l \Phi_i(\xi) \quad (21b)$$

Upon computing of the global diffusion matrix  $[\mathbf{A}]$ , the global mass matrix  $[\mathbf{B}]$  and the global force vector  $\mathbf{F}$  by assembling the elemental values defined in Eq. (19), a semi-discrete tridiagonal head-based system of  $N$  nonlinear algebraic equations is obtained. In general, the mass matrix  $[\mathbf{B}]$  in the discretized head-based equation causes a major problem such as a possible numerical oscillation and convergence problem when the distributed mass matrix is used to approximate Eq. (19). Moreover, it has been demonstrated that the diagonal mass cumulative results are superior to the mass distributed one in the pressure-based equation. In fact, the lumped mass scheme converges rapidly. The mass lumping formulation provides an excellent mass balance error compares to the solution obtained using the mass distributed matrix in pressure based which can provide different numerical solutions [15, 44]. Therefore, the mass lumping approach is used in this study. Different temporal discretization schemes of Eq. (19) can be adopted and discuss in the literature [45, 46]. Three temporal discretization schemes will be considered in this study: two level finite difference scheme with and without standard chord slope (SCS) and three-level finite difference scheme. These finite differential schemes will be coupled with the Picard iteration method which involves sequential prediction of parameter and variables at the latest known. For the two-level forward finite difference scheme also referred in the literature as the Euler or the tangent scheme, the finite differential of Eq. (19)

gives

$$[\mathbf{A}]\Psi^{k+1,m+1} + [\mathbf{B}]\left\{\frac{\Psi^{k+1,m+1} - \Psi^k}{\Delta t}\right\} = \mathbf{F} \quad (22)$$

where  $k$  represents the time level,  $m$  is the previous iteration level and  $\Delta t = t^{k+1} - t^k$  is the time step between the latest and the old time. For two-level finite difference scheme which presents a first order truncation error, two formulations of the element specific moisture capacity are considered. In the first formulation designed as two-level scheme, the specific moisture capacity is computed analytically and evaluated at the latest time and old Picard iteration. For the second formulation designed as the standard chord slope (SCS), the specific moisture capacity at the latest time and old Picard iteration is evaluated by the relation

$$C^{k+1,m} = \frac{\eta^{k+1,m} - \eta^k}{\Psi^{k+1,m} - \Psi^k} \quad (23)$$

It can be noted that the standard chord slope uses moisture content  $\eta^{k+1,m}$  and pressure-head  $\Psi^{k+1,m}$  at the latest time and previous Picard iteration. For the three-level finite difference scheme known as the second order truncation error, the specific moisture capacity is evaluated at the latest time and previous Picard iteration. The implicit discretized equation is then expressed as

$$[\mathbf{A}]\{\Psi\}^{k+1,m+1} + [\mathbf{B}]\left\{\frac{3\Psi^{k+1,m+1} - 4\Psi^k + \Psi^{k-1}}{2\Delta t}\right\} = \mathbf{F} \quad (24)$$

In order to solve Eqs. (22) and (24) using the Picard iteration method, the pressure head variable is transformed using the dependent variable  $\delta_j^{k,m} = \Psi_j^{k+1,m+1} - \Psi_j^{k+1,m}$  and the obtained equations can be written in the matrix form

$$\mathbf{M}^m \delta^m = \mathbf{R}^m \quad (25)$$

where  $\mathbf{M}$  is the tridiagonal matrix and  $\mathbf{R}$  the residual vector. In the computation procedure, known  $\Psi_j^k$  or  $\Psi_j^{k+1,m}$  is assigned to the unknown pressure head  $\Psi_j^{k+1,m+1}$  and Eq. (25) is solved to obtain  $\Psi_j^{k+1,m+1}$ . Then, the moisture content  $\eta_j^{k+1,m+1}$  can be calculated using the fitting procedure. The pressure head  $\Psi_j^{k+1,m+1}$  is iteratively updated using the formula  $\Psi_j^{k+1,m+1} = \Psi_j^{k+1,m} + \varpi \delta_j^{k,m}$ , where  $\varpi$  is the weighting factor which is taken equal to 1 in this study. The convergence is achieved when the difference between pressure head values at two consecutive iteration levels satisfies a given criterion  $\max |\Psi_j^{k+1,m+1} - \Psi_j^{k+1,m}| < 0.01 \text{ cm}$ .

The mass balance error of the proposed spectral element method is evaluated by

$$MBE(t) = 100|1 - MB(t)| \quad (26)$$

where  $MB(t)$  is the mass balance which can be expressed as [15, 18]

$$MB(t) = (M_t - M_0) / \sum_{\Delta t} F_{\Delta t} \quad (27)$$

Here  $M_t$  is the mass storage at time  $t$ ,  $M_0$  represents the initial mass storage at the initial time, and  $F_{\Delta t}$  defined the mass entering the computation domain during the time step  $\Delta t$ .

## 4 Result and discussion

The cases studied consist of water flow through soil layers full of heterogeneities which can be approximated to one-dimensional transient flow processes. The flow can be oriented in the horizontal ( $\lambda = 0$ ), the vertical upward ( $\lambda = 1$ ), and the vertical downward ( $\lambda = -1$ ) directions. The initial and boundary conditions are assumed to be constant pressure head. This problem can be characterized by Eqs. (1-4) and the spectral element method as formulated in section 3 was used for the analysis. The integrations over an element were accomplished using two end-nodes upon the Legendre Gauss-Lobatto quadrature rule that generates the exact diagonal mass matrix which greatly simplifies the implementation algorithm. The spectral element method spatial domain was discretized in  $N = 41$  nodes and numerical predictions were implemented in MATLAB computer language in a machine equips with an Intel(R) Core™ i3, 2.40 GHz system.

For the primary problem, the moisture content and the hydraulic conductivity of unsaturated soil are given by Gardner [39] hydraulic characteristics defined by Eqs. (6) and (7). The soil is composed of sand and the corresponding data of this problem are  $\alpha = 1.611 \times 10^6$ ,  $\beta = 3.96$ ,  $\rho = 1.175 \times 10^6$ ,  $\gamma = 4.74$ ,  $\eta_s = 0.368$ ,  $\eta_r = 0.102$ , and  $K_s = 0.00944 \text{ cm/s}$ . The initial condition for a 40 cm soil depth was considered  $\Psi(z, t = 0) = \Psi_i = -61.5 \text{ cm}$ . The applied boundary conditions were inhomogeneous with the top of the soil column  $\Psi(z = 0 \text{ cm}, t) = \Psi_0 = -20.7 \text{ cm}$  and the bottom of the soil level  $\Psi(z = 40 \text{ cm}, t) = \Psi_L = -61.5 \text{ cm}$ . For this problem, an exact analytical solution of the pressure head distribution in the soil can be derived after the linearization of flow equation by performing the Kirchhoff transformation and using the method of separation of variables and the Fourier transform approach as

$$\Psi = \frac{1}{v} \ln \left[ (e^{v\Psi_L} - \varepsilon) e^{-\frac{\lambda v}{2}(z-L)} \Gamma + \varepsilon \right] \quad (29)$$

where

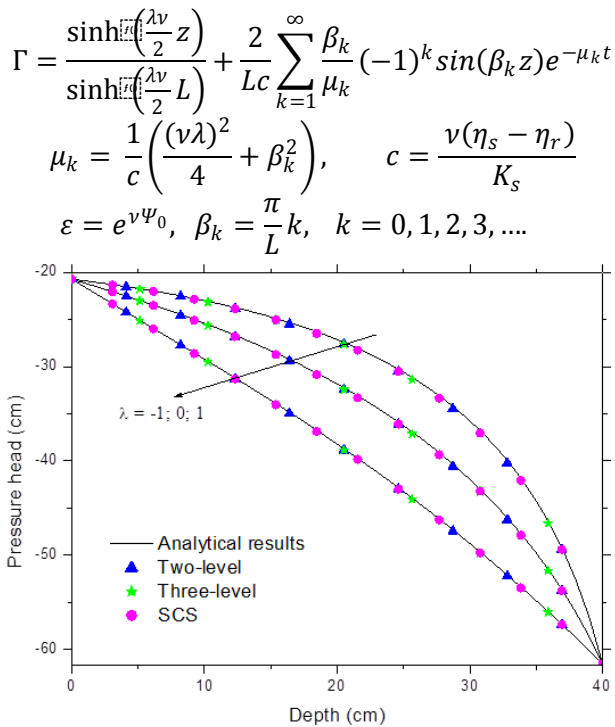


Fig.1. Comparison between spectral element and analytical results for three soil orientations and using a Gardner [39] hydraulic characteristics at  $t = 360s$  for  $\nu = 0.04$  and  $h_l = 1cm$

The distribution of pressure head versus the soil depth is shown in Fig. 1 for different time schemes at  $t = 360$  seconds and the pore distributed parameter  $\nu = 0.04$  for three soil water flow orientations: horizontal, vertical downward and upward. The current spectral element method predictions are compared to analytical results obtained with 5001 terms of the Fourier series. For numerical predictions, spatial domain discretized is constructed with a uniform spectral space  $h_l = 1cm$  and the constant time steps  $\Delta t = 1s$  which will be used as dense grid for the three temporal schemes: two-level with and without SCS; and three-level scheme. Excellent agreement is achieved between the present spectral element solution and the analytical results using three time approaches. This demonstrates the good efficiency of the spectral element method and implies that the three different temporal discretization schemes can be conveniently used for water flows analysis in unsaturated soils using the pressure head form of the Richards flow equation. It can be concluded from Fig. 1 that the selected temporal schemes have similar results for dense grid temporal discretization.

For the second problem, the soil hydraulic conductivity and moisture content are given by Haverkamp et al. [41] hydraulic characteristics of dry soil as defined by Eqs. (8) and (9). For soils

with these characteristics, the problem is nonlinear and the development of an exact analytical solution is difficult. In such case, the prediction of the spectral element method using dense grid will be used for reference solution as is generally encountered in the literature for finite element and finite difference methods [15, 18, 47]. The pressure head profiles in case of vertical downward soil infiltration ( $\lambda = -1$ ) and for three time discretization schemes are presented in Fig. 2. This figure shows that the soil pressure distribution decreases with increasing the soil depth until the wetting front where it remains constant. It can be seen in Fig. 2 that the time step of the temporal discretization scheme influences the SEM accuracy. As the time step  $\Delta t$  increases, the SEM pressure head predictions using the two- and three-levels schemes underestimate the soil water movement. It can be noted that the SEM pressure head predictions using SCS is less influence by the time step of the temporal discretization scheme: a time  $\Delta t = 30s$  is sufficient for predictions with acceptable accuracy: the maximum deviation from the reference solution is less than 2%. This good behavior of the SCS is confirmed when compare the three temporal discretization schemes for horizontal and vertical upward and downward water flow curves at  $t = 360s$ . For a time step  $\Delta t = 10s$ , the SCS numerical model gives good predictions of the soil pressure distribution for the three soil orientations considered while difference appears in the numerical predictions using two and three-levels schemes: the maximum deviation is 7% and 0.1% for predictions using two and three-levels schemes, respectively. The results of the present SEM formulation are also compared with the authors' finite element method (FEM) results. Two formulations of the FEM are considered: the finite element method (FEM) where standard formulation uses the simple two level finite difference temporal scheme and a modified finite element method (MFEM) with mass-lumped approximation. It should be noted that Celia et al. [15] have performed the MFEM for this problem. In Fig. 3, the predicted pressure head for  $\Delta t = 10s$  using SEM and FEM/MFEM are compared with the dense grid prediction considered as reference solution. Two observations are relevant. Firstly, predictions from the three numerical methods have a good qualitative agreement as all the three show the same trend of pressure head. Secondly, unlike the excellent behavior between the SEM and MFEM/FEM results, the two-level scheme slightly underpredicts the dense grid reference solution. These indicate that for small time stepping, spatial discretization

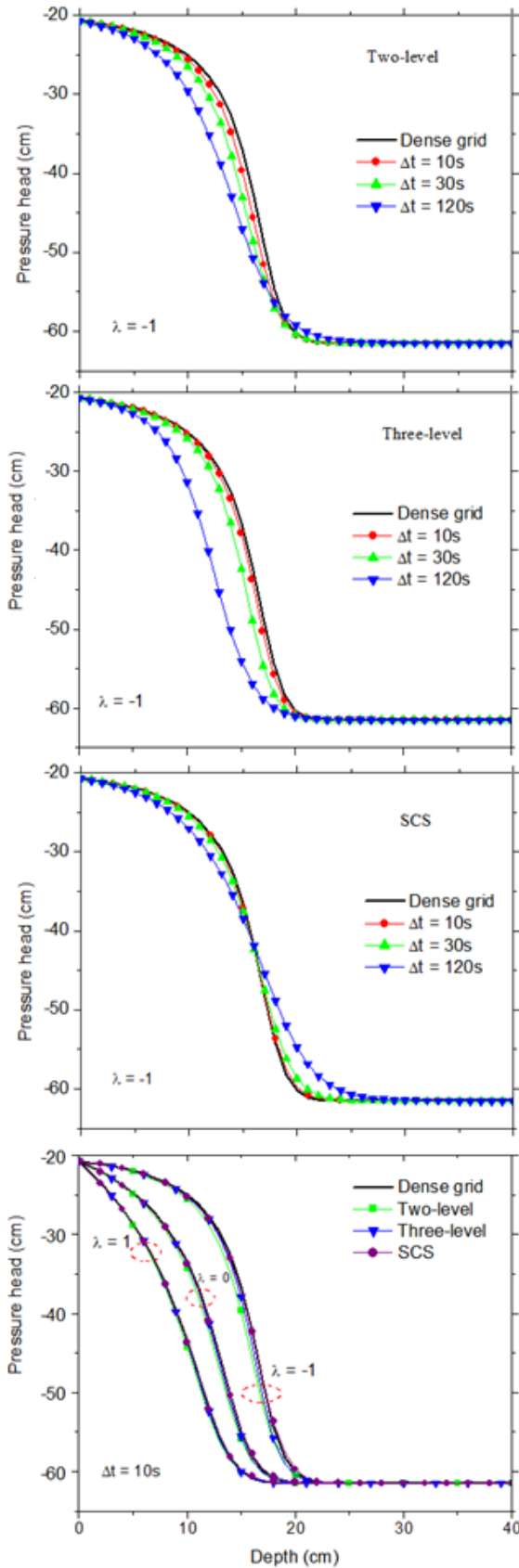


Fig.2. SEM pressure head predictions for the two-level, the three-level and the SCS temporal schemes for Haverkamp et al. [41] hydraulic characteristics at  $t = 360s$  and  $h_l = 1cm$ .

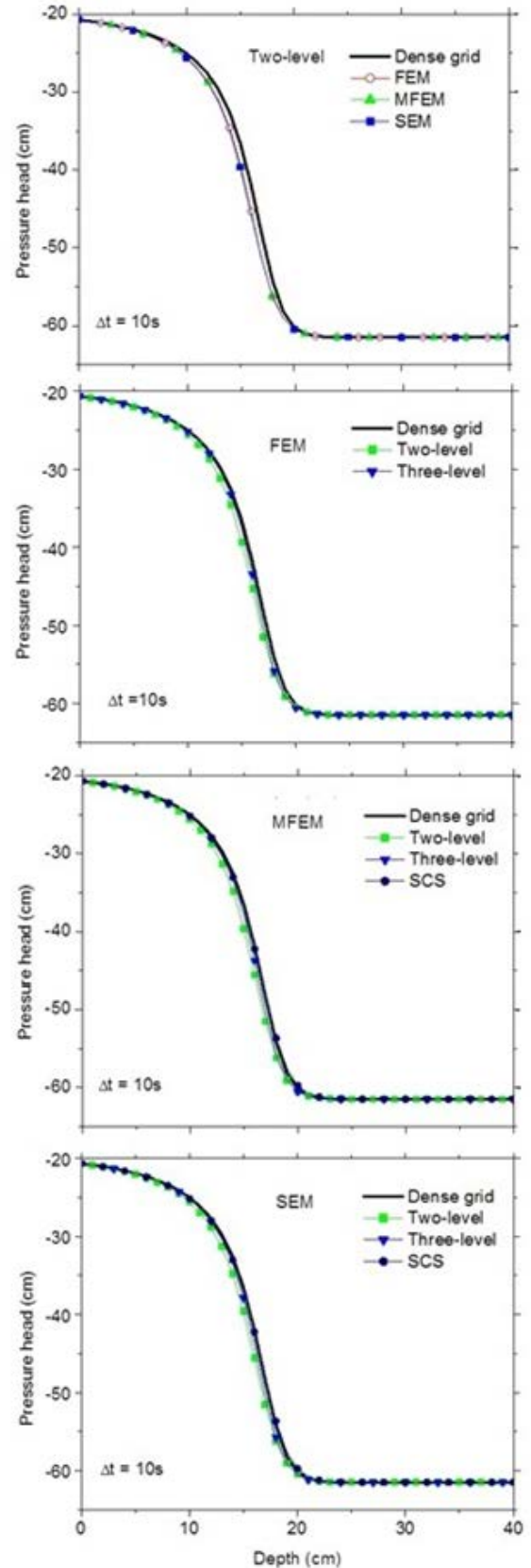


Fig.3. Comparison of FEM, MFEM and SEM solution using Two-level, Three-level and SCS approximations in case of vertical downward infiltration and for Haverkamp et al. [41] hydraulic characteristics.

scheme with high truncation order is suitable and that the evaluation of specific moisture capacity at the latest time and old Picard iteration as developed in the SCS scheme enhances the performance of low order truncation error scheme. This conclusion is supported by a far more comprehensive comparison between the three time discretization schemes based on the mass balance error and reported in the next subsection.

The performance of the SEM for the second problem is further access by evaluating the mass balance error; the results are shown in Figs. 4 and 5. The mass balance error in the SEM using two- and three-level schemes for various time steps and for vertical downward ( $\lambda = -1$ ), horizontal ( $\lambda = 0$ ), and vertical upward ( $\lambda = 1$ ) infiltrations are illustrated in Fig. 4. It can be seen that mass balance errors for the predictions using two- and three-level schemes exhibited similar behavior. The greatest mass balance errors occurred early in the simulation and converged towards zero as the value of time increases. With an increase of the time step  $\Delta t$ , the error in the solution increases leading to a poor mass balance; and an underestimation of infiltration depth is noted. It is clear from Figs. 4 that SEM pressure head predictions using the two-level scheme are greatly influence by the value of time step of the temporal discretization scheme than in predictions using three-level scheme. The maximum error on mass balance is observed for vertical upward and  $\Delta t = 30s$  is 12.6% for the two-level scheme while this error is less than 11.9% for the three-level scheme. This behavior is confirmed for prediction using dense grid that is  $\Delta t = 1s$ : the maximum errors are 1.9% and 0.4% for two- and three-level schemes, respectively. In fact, the magnitude of the mass balance correlates with the mass balance error and is generally influenced by both time and space meshes: The comparison of mass balance errors of the SEM using very small time and space discretization for vertical downward infiltration is presented in Fig. 5. This figure presents a better behavior of the prediction for three-level scheme to preserve mass balance error than in the case of two-level scheme. Fig. 5 also shows that the mass error on SEM pressure head predictions using SCS is zero and therefore this scheme is mass conservative. In Fig. 6, the mass balance errors between SEM and FEM/MFEM for a time step  $\Delta t = 10s$  are compared. Agreement is seen to be good between the SEM and the MFEM results. It is of interest to see that the mass balance error for these two methods for predictions using SCS is zero. This indicates that both SEM and MFEM using SCS scheme are mass conservative.

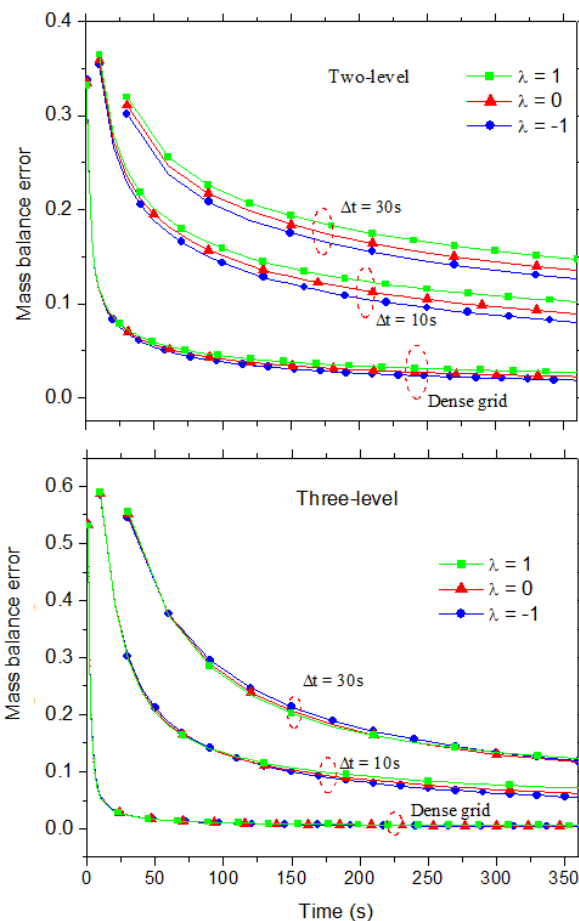


Fig.4. Mass balance error in the spectral element solution using two- and three-level schemes for various time steps and for vertical downward ( $\lambda = -1$ ), horizontal ( $\lambda = 0$ ), and vertical upward ( $\lambda = 1$ ) infiltrations for Haverkamp et al. [41] hydraulic characteristics

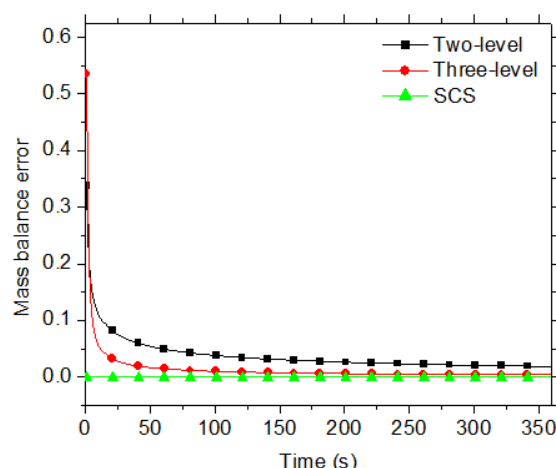


Fig.5. Mass balance error in the Spectral element solution for Haverkamp et al. [41] properties and using Two-level, Three-level and SCS approximations for dense grid and for vertical downward ( $\lambda = -1$ ) at  $t = 360s$ .

It can also be seen in Fig. 6 that for long times, numerical method using three-level scheme performed better than when using two-level scheme. In fact, high order schemes such as the three-level require previous knowledge on the lower scheme approximation and therefore improve solution accuracy. Still on Fig. 6, the FEM presents a better mass balance error that SEM and MFEM for predictions using the two-level scheme. However, this method is not conservative as the mass balance error is different from zero. The mass balance error, the cumulative error and the computational time for this second test problem using Haverkamp et al. [41] hydraulic soil characteristics is shown in Table 1 for various time steps. It can be noticed from Table 1 that the three temporal discretization schemes contribute to an increase in the cumulative mass error with time step. The SEM with two-level scheme presents the highest cumulative mass error while the lowest error is obtained for SEM using SCS. This is in agreement with previous findings on the three spatial discretizations. It can be noted in Table 1 that the FEM is almost non-conservative. In fact, the accuracy the FEM decreases with increases time steps with the least mass balance error of 0.06 for time steps equal 10s. However, FEM is more accurate than MFEM and SEM using the simple two level finite difference temporal scheme. Similar conclusions are noted for predictions using three-level temporal scheme. In contrast, when standard chord slope is used for temporal discretization, the FEM did not converge while MFEM and SEM are mass-conservative. The maximum mass balance errors for MFEM and SEM are less than  $3 \times 10^{-5}$  and increases with increasing time step. The capacity to distinguish between various methods is also analyzed in term of the time necessary to compute the pressure head of the flow equation. The so call CPU or computational time is evaluated in this study as the sum of pre-processing and processing simulation times. As presented in Table 1, computational time for SEM standard chord slope scheme is less than for MFEM for small time steps. Therefore, the SEM appears to be more computational efficient than the finite element methods. Table 1 shown that computation was conducted in less than 1s, meaning that the SEM presents a very small simulation time. Table 1 also shows that the difference in the simulation time between FEM and SEM/MFEM becomes smaller with increase of the time step numbers. This can be explained by the fact the FEM used the distributed mass matrix while the SEM/MFEM is implemented with the mass lumping matrix. The distributed mass matrix induced more iteration steps for the

convergence and therefore more computational time for FEM as the time step is refined.

Table 1. Mass balance errors and computational times in the SEM for various time discretization schemes at  $t = 360s$  and  $\Delta z = 1cm$  for vertical downward infiltration using Haverkamp et al. [41] dry soil characteristics.

Scheme	Time steps (s)	Mass Balance			Mass Balance error			CPU time (s)		
		FEM	MFEM	SEM	FEM	MFEM	SEM	FEM	MFEM	SEM
Two-level	10	0.934	0.919	0.919	0.066	0.080	0.080	1.766	1.031	0.250
	30	0.882	0.874	0.874	0.118	0.126	0.126	0.719	0.625	0.156
	120	0.814	0.811	0.811	0.186	0.186	0.189	0.469	0.328	0.109
Three-level	10	0.964	0.945	0.945	0.036	0.055	0.055	1.719	0.844	0.469
	30	0.896	0.881	0.881	0.104	0.119	0.119	0.734	0.516	0.375
	120	0.713	0.707	0.707	0.287	0.293	0.293	0.469	0.344	0.203
SCS	10	-	1.000	1.000	-	$2.533 \times 10^{-5}$	$2.534 \times 10^{-5}$	-	1.016	0.500
	30	-	1.000	1.000	-	$1.359 \times 10^{-5}$	$1.359 \times 10^{-5}$	-	0.672	0.344
	120	-	1.000	1.000	-	$4.909 \times 10^{-6}$	$4.926 \times 10^{-6}$	-	0.359	0.297

For the third problem, an infiltration into an unsaturated and very dry soil column with hydraulic characteristics, given by van Genuchten [42] model as defined by Eqs. (10) and (11) was considered. The parameters used by this model are:  $\alpha = 0.0335$ ,  $\eta_s = 0.368$ ,  $\eta_r = 0.102$ ,  $n = 2$ ,  $m = 0.5$ ,  $K_s = 0.00922 cm/s$ . The initial condition was taken as  $\Psi(z, t = 0) = \Psi_i = -1000cm$ . The Dirichlet boundary conditions were imposed at the top soil surface and at the bottom level as  $\Psi(z = 0cm, t) = \Psi_0 = -1000cm$  and  $\Psi(z = 100cm, t) = \Psi_L = -75cm$ . A similar numerical analysis as for the second problem is carried out. However, the total computational time is 86400s; the node constant spacing is assumed to be  $h_l = 2.5cm$ . The larger number of time nodes for this problem required more computational time. Fig. 7 shows the variation of the downward pressure head at  $t = 86400s$  versus soil depth using the three-level, the two-level with and without SCS temporal schemes discretization. A more pronounce variances are noted between in the three spatial time discretization schemes. The SCS converges for five time steps discretization having the following values:  $\Delta t = \{20, 120, 144, 720, 3600\}s$  and dense grid. This confirms a better performance of the SCS for pressure head flow in a very dry soil with hydraulic characteristics given by van Genuchten [41] model. As illustrated in Fig. 7, the SEM pressure head predictions using the two-level scheme for time step values greater than  $\Delta t = 20s$  are found to be less accurate than prediction using dense grid scheme and did not converge for  $\Delta t = 144s$  which is not represented. Still in Fig. 7, the SEM pressure head predictions using three-level scheme has been

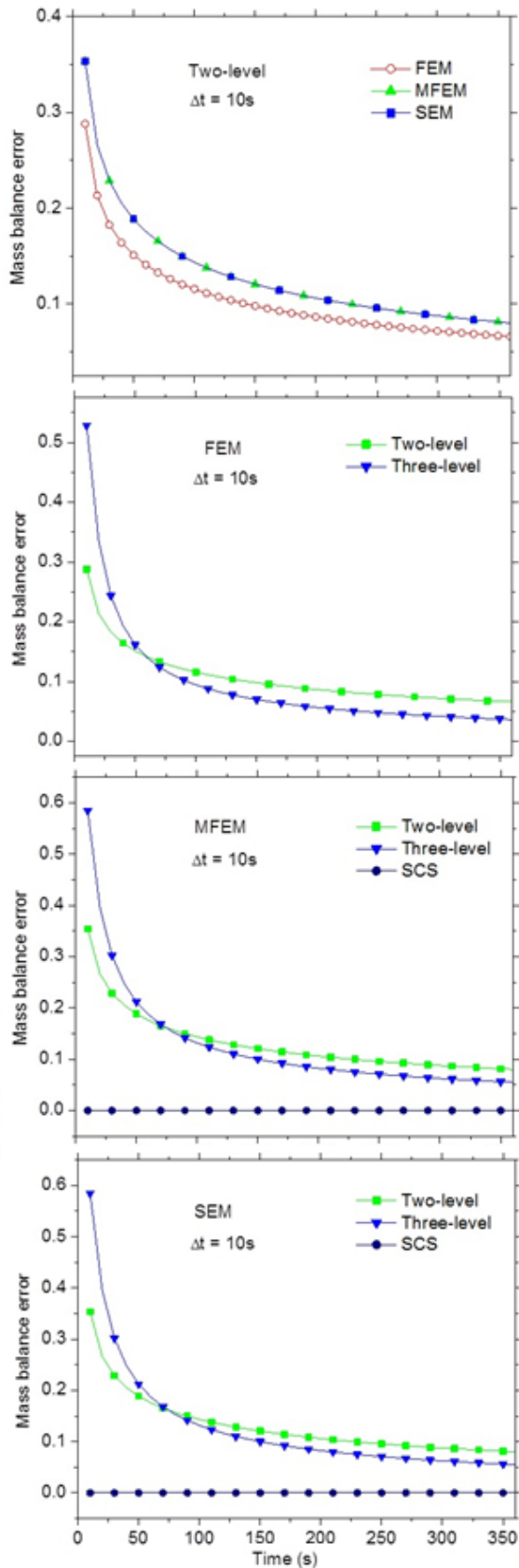


Fig.6. Comparison of FEM, MFEM and SEM mass balance error using Two-level and Three-level approximations in case of vertical downward infiltration at  $t = 360s$ .

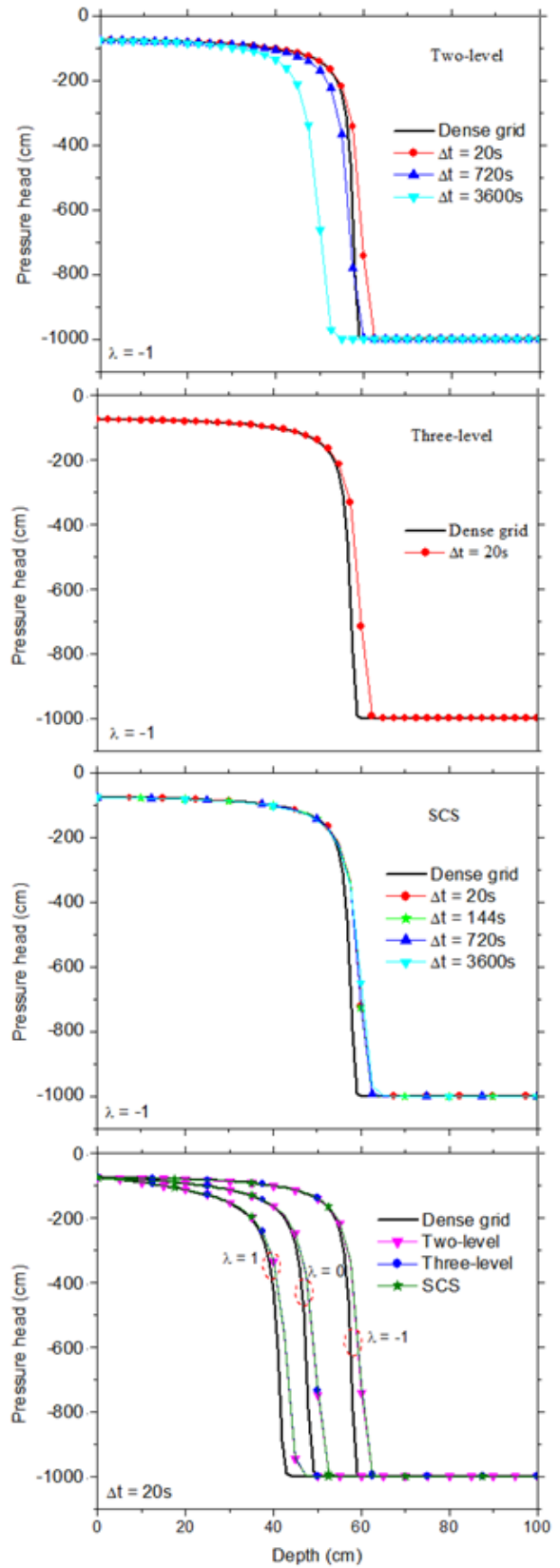


Fig.7. SEM pressure head predictions for the two-level, the three-level and the SCS temporal schemes for van Genuchten [42] hydraulic characteristics at  $t = 86400s$  and  $h_l = 2.5cm$ . illustrated only for  $\Delta t = 20s$  since this scheme did

not converge for time steps greater than this value. This leads to conclude that the solution of unsaturated flow processes in very dry soil with hydraulic characteristics given by van Genuchten [42] model requires refined time meshes for accurate predictions. In addition of the effect of time step discretization on the accuracy of SEM, Fig. 7 illustrates SEM pressure head predictions for vertical downward ( $\lambda = -1$ ), horizontal ( $\lambda = 0$ ), and vertical upward ( $\lambda = 1$ ) infiltrations at  $t = 86400s$ . For each case, the pressure head predictions are found to be accurate compared with the reference solution obtained using a dense grid discretization. The maximum deviations between predictions using two-level and three-level schemes are  $2.2 \times 10^{-1}\%$  and  $3 \times 10^{-2}\%$ , respectively for pressure head predictions in vertical downward ( $\lambda = -1$ ) infiltrations. This confirms the analysis presented for the second problem. Figs. 8 show a comparison of the SEM and FEM/MFEM predictions using two-level, three-level and SCS approximations at time  $t = 86400s$ . Computations have been carried out for a time step  $\Delta t = 20s$  and in case of vertical downward infiltration. The agreements between SEM and MFEM predictions are excellent. As depicted in Figs. 8 and as were observed by Celia et al. [15], the FEM predictions presents numerical oscillations at the pressure head wetting front which is due to the highly nonlinear characteristics of moisture content capacity and hydraulic conductivity for this example. In fact, the spatial distribution of the time derivative term incorporated in the mass matrix when using the FEM for the discretized equation must be the major cause of this difference in numerical results.

The mass balance error for the third problem is illustrated in Fig. 9. This figure shows that the mass balance error of the SEM using two-level scheme increases with time step discretization. It can be seen that for  $\Delta t = 20s$ , the maximum mass balance error is obtained for vertical upward infiltration while the minimum is for vertical downward infiltration. These figures also shown that SEM with three-level scheme is more accurate than SEM with two-level scheme: the maximum error is less than 2% and 0.6% for two-level and three-level schemes, respectively. In addition, the SCS has better convergence than two-level and three-level schemes. The mass balance error for this scheme is zero meaning that this scheme is more mass conservative. Fig. 10 shows comparisons between the SEM and FEM/MFEM on the mass balance error at a time step  $\Delta t = 20s$ . As noted previously, a high order discretization scheme improves the

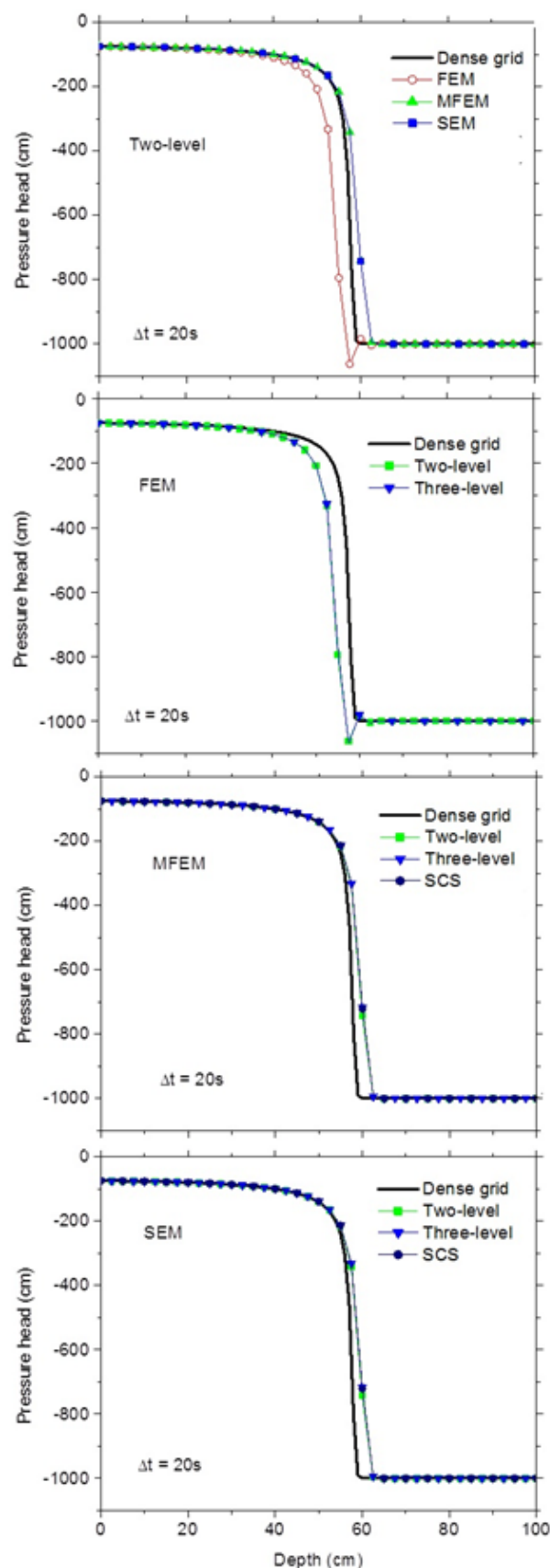


Fig.8. Comparison of FEM, MFEM and SEM solution using Two-level, Three-level and SCS approximations in case of vertical downward infiltration at  $t = 86400s$

solution accuracy whereas the evaluation of the specific moisture capacity at the latest time and old Picard iteration as use in SCS scheme enhances considerably the performance of low order time discretization. It can be seen in Fig. 10 that the SEM and MFEM present satisfactory mass balance errors for SCS scheme, whereas there are considerable errors in the FEM predictions. This disagreement is attributed to the fact that for this method, the specific moisture capacity cannot be evaluated at the latest time and old Picard iteration. This result is summarized in Table 2 where it can be seen that the SCS is more efficient than the two- and three-level schemes.

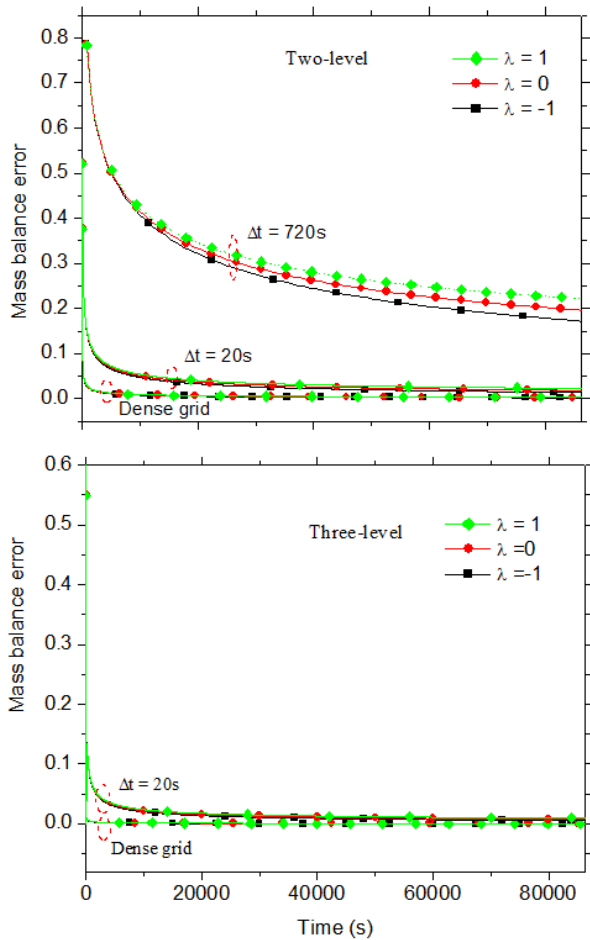


Fig.9. Mass balance error versus the time in case of Two-level and Three-level schemes, respectively and for various soil flow orientations for van Genuchten [42] properties.

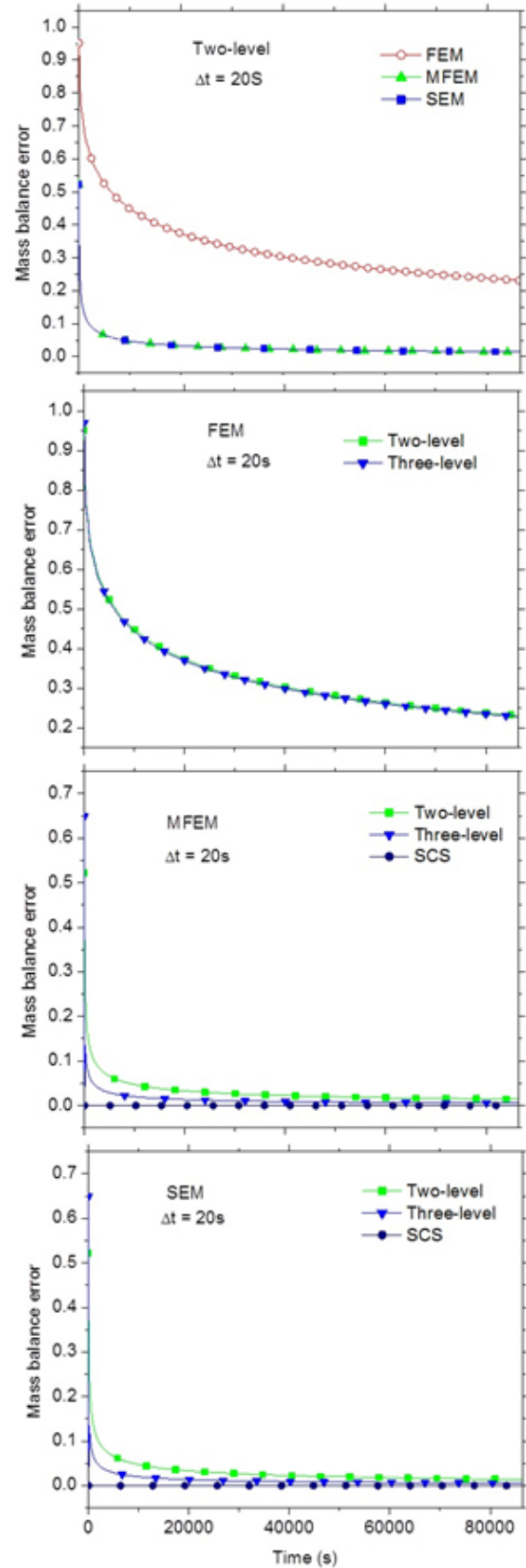


Fig.10. Comparison of FEM, MFEM and SEM mass balance error using Two-level and Three-level approximations in case of vertical downward infiltration at  $t = 86400s$ .

Table 2. Mass balance errors and computational times in the SEM for various time discretization schemes at  $t = 86400s$  and  $\Delta z = 2.5cm$  for vertical downward infiltration using van Genuchten [42] in very dry soil characteristics.

Scheme	Time steps (s)	Mass Balance			Mass Balance error			CPU time (s)		
		FEM	MFE M	SEM	FEM	MFE M	SEM	FEM	MFE M	SEM
Two-level	20	0.769	0.985	0.985	0.231	0.014	0.014	171.64	46.734	14.344
	144	0.752	-	-	0.248	-	-	32.781	-	-
	720	0.693	0.828	0.828	0.307	0.172	0.172	8.156	3.890	1.531
	3600	0.538	0.601	0.601	0.461	0.399	0.399	2.937	2.781	0.984
Three-level	20	0.772	1.005	1.005	0.228	0.005	0.005	191.70	38.953	12.969
	144	-	-	-	-	-	-	-	-	-
SCS	20	-	1.000	1.000	-	$2.433 \times 10^{-7}$	$2.434 \times 10^{-7}$	-	43.875	15.516
	144	-	1.000	1.000	-	$1.201 \times 10^{-7}$	$1.202 \times 10^{-7}$	-	9.250	3.187
	720	-	1.000	1.000	-	$8.591 \times 10^{-8}$	$8.581 \times 10^{-8}$	-	3.344	1.375
	3600	-	1.000	1.000	-	$9.849 \times 10^{-8}$	$9.824 \times 10^{-8}$	-	1.844	0.734

For  $\Delta t = 20s$ , Table 2 shows that the three time discretization schemes computational times are comparable. However, the SCS scheme produces an excellent mass balance and mass balance errors equal to zero. The three-level scheme with a mass balance equal to 1.005 and mass balance error of  $5.45 \times 10^{-3}$  performed better than the two-level scheme, where the mass balance is equal to 0.9857 and the mass balance error is 0.0143. These observations confirm the analysis presented in the case of the second problem describing pressure head flow in a dry soil with hydraulic characteristics given by Haverkamp et al. [41] model. Comparisons between the results obtained from SEM and authors' finite element methods results shows that the FEM is non-conservative for this test problem; the mass balance error is about 0.2 whereas, the mass balance error is about 0.01 for predictions using MFEM and SEM with the two-level time discretization scheme. A better accuracy of MFEM and SEM compare to FEM can also be observed when the standard chord slope is used for temporal discretization. As presented in Table 2, both MFEM and SEM with standard chord slope schemes are mass-conservative. Comparison of Table 1 and 2 reveals that the SEM and FEM/MFEM performances are crucially affected by the soil characteristics. A great difference can be noted on mass balance errors for infiltration into dry and very dry soils characterized by Haverkamp et al. [41] and van Genuchten [42], respectively. The mass balance error for FEM is generally similar to all other methods in Table 1, whereas in Table 2, SEM/MFEM has lower errors. The highly nonlinear and complex characteristics of the very dry soil considered in the third example combined to the distributed mass matrix considered

in the FEM explained the great difference of the mass balance errors between the three numerical methods. The spatial distribution of the time derivative term generates a major problem such as a possible numerical oscillation and convergence of the FEM. Table 2 also shown that the simulation time in the FEM solutions increases drastically for infiltration into an unsaturated soil subjected to very dry conditions. The MFEM converges rapidly compare to the FEM method and the effect of diagonalization of the mass matrix is more evident. It can be seen in Table 2 that the computational time of the MFEM for the mass-conservation model using standard chord slope scheme is greater than for the SEM for small time steps. Hence, the SEM is more efficient than finite element methods for water flow in unsaturated porous soils where hydraulic characteristics are highly nonlinear.

## 5 Conclusion

A spectral element method for the analysis of flows in unsaturated soils is presented. The method is based on Legendre Gauss-Lobatto quadrature sets for spatial discretization while temporal discretization is achieved by the Picard iteration procedure for soil moisture linearization combined with fully implicit time two-level with and without standard chord slope and three-level discretization schemes. The analyses were performed for pressure head flow in horizontal, upward and downward vertical unsaturated soils and for various hydraulic characteristics. The numerical experiments demonstrate that the spectral element method can be used to achieve accurate mass balance predictions and is a rapid convergent algorithm with less computational time. The major conclusions are as follows:

- the spectral element method agrees to exact result for hydraulic characteristics presented by the Gardner [39] model;
- for unsaturated soils with highly nonlinear hydraulic characteristics given by Haverkamp et al. [41] and van Genuchten [42] models, the spectral element method using standard chord slope scheme is mass conservative, while using three-level scheme and standard two-level schemes is mass conservative for time steps refinement;
- The spectral element method using three-level scheme is more accurate than using the standard two-level scheme.
- The spectral element method is computational more efficient than finite element methods for

water flow in unsaturated porous soils where hydraulic characteristics are highly nonlinear.

These improved transient water flow predictions for unsaturated soils with variable coefficients are significant for remote sensing of soil-plant-atmosphere as well as in soil pressure head modeling efforts. The limitations of the present study include its one-dimensionality. However, since the spectral element method has proven to be a robust, accurate, convergent and conservative numerical method of the one-dimensional transient water flow in unsaturated soil, it is expected that the method may be applied in the future in multi-dimensional flow problem. Developing and implementing such multi-dimensional spectral element method will be useful for the investigation of the horizontal soil moisture heterogeneity and atmosphere boundary effects. The present study using the SEM for one-dimensional transient water flow in unsaturated soil sets the basis for such future investigations.

### Acknowledgment

E.L.L., H.T.T.K. and E.H.Z.T. acknowledge the Volkswagen Foundation through grant number VW 89362 under the funding initiative Knowledge for Tomorrow- Cooperative Research Project in sub-Saharan Africa on Resource, their Dynamics, and Sustainability.

### References:

- [1] Berg, P., Long-term simulation of water movement in soils using mass-conserving procedure, *Advances in Water Resources*, Vol. 22, 1999, pp. 419-430.
- [2] Bitteli, M., Ventura, F., Campbell, G.S., Snyder, R.L., Gallegati, F. and Pisa, P.R., Coupling of heat, water vapor, and liquid water fluxes to compute evaporation in bare soils, *Journal of Hydrology*, Vol. 362, 2008, pp. 191-205.
- [3] Carbone, M., Brunetti, G. and Piro, P., Modelling the hydraulic behavior of growing media with the explicit finite volume solution, *Water*, Vol. 7, 2015, pp. 568-591.
- [4] Nimmo, J.R., Unsaturated Zone Flow Processes, in Anderson MG, and Bear J., eds *Encyclopedia of Hydrological Sciences: Part 13-Groundwater*: Chichester, UK, Wiley, Vol. 4, 2005, pp. 2299-2322.
- [5] Chotpantararat, S., Limpakanwech, C., Siriwong, V., Siripattanakul, S. and Sutthirat, C., "Effect of soil water characteristic curves on simulation of nitrate vertical transport in a Thai agricultural soil", *Sustain. Environ. Res.*, Vol. 21, 2011, pp. 187-193.
- [6] Ogden, F.L., Lai, W., Steinke, R.C., Zhu, J., Talbot, C.A. and Wilson, J.L., A new general 1-D Vadose zone flow solution method, *Water Resour. Res.*, Vol. 51, 2015, pp. 1-19.
- [7] Ritsema, C.J., Dekker, L.W., Hendrickx, J.M.H. and Hamminga, W., Preferential flow mechanism in a water repellent sandy soil, *Water Resour. Res.*, Vol. 29, 1993, pp. 2183-2193.
- [8] Saito, H., Simunek, J., Mohanty, B.P., Numerical analysis of coupled water, vapor, and heat transport in the vadose zone, *Vadose Zone J.*, Vol. 5, 2006, pp. 784-800.
- [9] Davary, K., Ghahraman, B. and Sadeghi, M., Review and classification of modeling approaches of soil hydrology processes'', *Iran Agricultural Research*, 2007, Vol. 25, p. 2 and Vol. 26, pp. 1-2.
- [10] Sheng, D., Gens, A., Fredlund, D.G. and Sloan, S.W., Unsaturated soils: from constitutive modelling to numerical algorithms, *Computers and Geotechnics*, Vol. 35, 2008, pp. 810-824.
- [11] Liu, B.C., Liu, W. and Peng, S.W., Study of heat and moisture transfer in soil with dry surface layer, *International Journal of Heat and Mass Transfer*, Vol. 48, 2005, pp. 4579-4589.
- [12] Richards, L.A. Capillary conduction of liquids through porous mediums, *Physics*, Vol. 1, 1931, pp. 318-333.
- [13] Lee, D.H. and Abriola, L.M. Use of the Richards equation in land surface parameterizations, *J. Geophys. Res.*,104(D22), 1999, pp. 27519-27526.
- [14] Allen, M.B. and Murphy, C.L. A finite element collocation method for variably saturated flow in two space dimensions, *Water Resour. Res.*, Vol. 22, 1986, pp. 1537-1542.
- [15] Celia, M.A., Bouloutas, E.T. and Zarba, R.L. A general mass-conservative numerical solution for the unsaturated flow equation, *Water Resour. Res.*, Vol. 26, 1990, pp.1483-1496.

- [16] Milly, P.C.D. A mass-conservative procedure for time stepping in models of unsaturated flow, *Advances in Water Resources*, Vol. 8, 1985, pp. 32-36.
- [17] Vasconcellos, C.A.B. and Amorim, J.C.C., Numerical simulation of unsaturated flow in porous media using a mass-conservative model'', *Proc COBEM Fluid Mech*; Vol. 8, 2001, pp. 139-148.
- [18] Rathfelder, K. and Abriola, L.M., Mass conservative numerical solutions of the head-based Richards equation, *Water Resources Research*, Vol. 30, 1994, pp. 2579-2586.
- [19] Varado, N., Braud, I., Ross, P.J. and Haverkamp, R., Assessment of an efficient numerical solution of the 1D Richards equation on bare soil, *J. Hydrol.*, Vol. 323, 2006, pp. 244-257.
- [20] Radu, F. A., Pop, I. S., Attinger, S., and Knabner, P., Error estimates for an Euler implicit-mixed finite element scheme for reactive transport in saturated/unsaturated soil, *Proc. Appl. Math. Mech.* 7, 2007, 1024705-1024706.
- [21] Badruddin, I.A., Khan, A., Idris, M.Y.I., Nik-Ghaali, N., Salman Ahmed N.J. and Al-Rashed, A.A.A.A., Simplified finite element algorithm to solve conjugate heat and mass transfer in porous medium, *International Journal of Numerical Methods for Heat & Fluid Flow*, Vol. 27, Issue: 11, 2017, pp.2481-2507
- [22] Eymard, R., Gutnic, M., Hilhorst, D., The finite volume method for Richards equation'', *Comput. Geosci.*, Vol. 3, 1999, pp. 259-294.
- [23] Patera, A.T., A spectral element method for fluid dynamics laminar flow in a channel expansion, *Journal of Computational Physics*, Vol. 54, 1984, pp. 468-488.
- [24] Schrefler, B.A., Zhan, X. and Simoni, L., A couple model for water flow, airflow and heat flow in deformable porous media, *International Journal of Numerical Methods for Heat & Fluid Flow*, Vol. 5, 1995, pp. 531-547.
- [25] Stelzer, R. and Hofstetter, G., Adaptive finite element analysis of multiphase problems in geotechnics, 2005, *Computers and Geotechnics*, Vol. 32, pp. 458-481.
- [26] Trefethen, L.N. *Spectral Methods in MATLAB*, Society for Industrial and Applied Mathematics (SIAM), Philadelphia, PA, 2000.
- [27] Komatitsch, D., Bornes, C. and Tromp, J., Wave propagation near a fluid solid interface: A spectral-element approach, *Geophysics*, Vol. 65, 2000, pp. 623-631.
- [28] Shamsi, M., Modified pseudo spectral scheme for accurate solution of Bang-Bang optimal control problems, *Optim. Control. Appl. Mat.*, Vol. 32, 2011, pp. 668-680.
- [29] Ben-yu Guo, Jie Shen and Chen-long Xu Spectral and pseudo-spectral approximations using Hermite functions: application to the Dirac equation, *Advances in computational Mathematics*, Vol. 19, 2003, pp. 35-55.
- [30] Chen, M.J., Borthwick, A.G.L. and Eatock Taylor, R., Pseudospectral element model for free surface viscous flows, *International Journal of Numerical Methods for Heat & Fluid Flow*, Vol. 15, 2005, pp. 517-554.
- [31] Dehghan, M. and Sabouri, M., A Legendre spectral element method on a large spatial domain to solve the predator-prey system modeling interacting populations, *Applied Mathematical Modelling*, Vol. 37, 2013, pp. 1028-1038.
- [32] El-Baghdady, G.I., El-Azab, M.S. and El-Beshbeshy, W.S., Legendre-Gauss-Lobatto-Pseudo-spectral Method for One-Dimensional Advection-Diffusion Equation, *Sohag. J. Math.*, Vol. 2, 2015, pp. 29-35.
- [33] Minjeaud, S. and Pasquetti, R., High Order C0-Continuous Galerkin Schemes for High Order PDEs, Conservation of Quadratic Invariants and Application to the Korteweg-de Vries Model, *J. Sci. Comput.* 2018, 74: 491.
- [34] Cantwell, C.D., Moxey, D., Comerford, A., Bolis, A., Rocco, G., Mengaldo, G., De Grazia, D., Yakovlev, S., Lombard, J-E., Ekelschot, D., Jordi, B., Xu, H., Mohamied, Y., Eskilsson, C., Nelson, B., Vos, P., Biotto, C., Kirby, R.M. and Sherwin, S.J., Nektar++: An open-source spectral/hp element framework, *Computer Physics Communications*, Vol. 192, 2015, pp. 205-219.
- [35] Strebel, L., A groundwater and runoff formulation for weather and climate models,

*Journal of Advances in Modeling Earth Systems*, Vol. 10, 2018, pp. 1809-1832.

- [36] Vanderborght, J., Fetzer, T., Mosthaf, K., Smits, K.M., and Helmig, R., Heat and water transport in soils and across the soil-atmosphere interface: 1. Theory and different model concepts, 2017, *Water Resources Research*, Vol. 53, pp. 1057-1079.
- [37] Deng, Z., Guan, H., Hutson, J., Forster, M.A., Wang, Y. and Simmons, C.T., A vegetation-focused soil-plant - atmospheric continuum model to study hydrodynamic soil-plant water relation, *Water Resources Research*, Vol. 53, 2017, pp. 4965-4983.
- [38] Abdellatif, N., Bernardi, C., Touihri, M. and Yakoubi, D., A priori error analysis of the implicit Euler, spectral discretization of a nonlinear equation for a flow in a partially saturated porous media, *Adv. Pure Appl. Math.* Vol. 9(1), 2018, pp. 1–27.
- [39] Gardner, W., Some steady-state solutions of the unsaturated moisture flow equation with application to evaporation from a water table, *Soil Science*, Vol. 85, 1958, pp. 228-232.
- [40] Huang, R.Q. and Wu, L.Z., Analytical solutions to 1-D horizontal and vertical water infiltration in saturated/unsaturated soils considering time varying rainfall, *Computers and Geotechnics*, Vol. 39, 2012, pp. 66-72.
- [41] Haverkamp, R., Vauclin, M., Touma, J., Wierenga, P.J. and Vachaud, G., A comparison of numerical simulation models for one-dimensional infiltration, *Soil. Sc. Soc. Am. J.*, Vol. 41, 1977, pp. 285-294.
- [42] van Genuchten, M.T., A closed form equation for predicting the hydraulic conductivity of unsaturated soil, *Soil. Sci. Soc. Am. J.*, Vol. 44, 1980, pp. 892-898.
- [43] Shen, J. and Tang, T., Spectral and high-order methods with applications, Science Press, Beijing, 2006.
- [44] van Genuchten, M.T., A comparison of numerical solution of the one-dimensional unsaturated-saturated flow and mass transport equations, *Advances in Water Resources*, Vol. 5, 1982, pp. 47-55.
- [45] Paniconi, C., Putti, M., A Comparison of Picard and Newton Iteration in the Numerical Solution of Multidimensional Variably Saturated Flow Problems, *Water Resources Research*, Vol. 30(12), 1994, pp. 3357-3374.
- [46] List, F., Radu, F. A., A study on iterative methods for solving Richards' equation, *Comput Geosci.*, Vol. 20, 2016, pp.341–353.
- [47] Shahraiyini, H.T. and Ataie-Ashtiani, B., Mathematical forms and numerical schemes for the solution of unsaturated flow equations, *Journal of Irrigation and Drainage Engineering*, Vol. 138, 2012, pp. 63-72.